ISSN : 0974 - 7486 Volume 9 Issue 2

Materials Science

Trade Science Inc.

An Indian Journal

Full Paper

MSAIJ, 9(2), 2013 [73-77]

Microstructure, indentation creep and mechanical properties of Sn-Sb rapidly solidified alloys

A.El-Bediwi*, K.M.Ismail, M.Kamal

Metal Physics Lab., Physics Department, Faculty of Science, Mansoura University, (EGYPT)

E-mail: Baker_elbediwi@yahoo.com

ABSTRACT

Microstructure, creep behavior, elastic modulus and internal friction of Sn_{100-x}–Sb_x (X=2.2, 10 and 50 wt.%) rapidly solidified alloys have been investigated. Creep behavior of Sn- Sb alloys was studied by long time Vickers indentation testing at room temperature. Stress exponent value of Sn- Sb alloys were determined using Mulheam–Tabor method. Exponents values of Sn- Sb alloys in the range of 5.48–12.57 which in good agreement with the values of Sn based alloys reported in the literature. Elastic modulus of Sn_{100-x}–Sb_x (X=2.2, 10 and 50 wt.%) rapidly solidified bearing solder alloys increased but internal friction decreased with Sb content increased.

KEYWORDS

Sn-Sb alloys;
Stress exponent;
Elastic modulus;
Internal friction.

INTRODUCTION

White metal is now widely used as a material for sliding bearings operating under oil lubrication, for example, bearing for general industrial use, marine use and automotive use. White metal can be fundamentally classified into two types. One has lead as its main component, the other tin. Tin base Babbitt commonly contain copper and antimony have higher hardness which gives them excellent load-carrying characteristics. They show low friction resistance, low wear, good run-in properties and good emergency behavior in the absence of adequate lubrication. They "wet" easily and maintain an oil film, resist corrosion, are easily cast and bonded and retain good mechanical properties at elevated temperatures. Tin has a low coefficient of friction, which is the first consideration in its use as a bearing material. The effect of solidification rate, heating and microadditions on microstructure, hardness and mechanical properties of tin-based white metals have been investigated[1,2]. Rapid cooling suppresses formation and growth of SbSn cuboids and increases hardness. Also heating makes the precipitate's corners, especially SbSn cuboids, round.

The elastic modulus, internal friction and stiffness values of quenched Sn-Sb bearing alloy have been evaluated using the dynamic resonance technique[3]. The correlation of structure with mechanical and electrical properties of Sn- Sb rapidly solidified alloys have been studied by several investigators[4- 8]. Creep behavior, elastic modulus and internal friction of $Sn_{86}Sb_{10}Cu_2X_2$ (X = Pb, Ag, Se, Cd and Zn) alloys have been investigated and stress exponent have determined using Mulhearn- Tabor method[9]. Creep behavior of Sn-5%Sb alloy was studied by long time Vickers indentation testing at room temperature and at temperatures in the range 298–405 K[10,11]. Annealing temperature affects the structure and properties of Sn- Sb alloy The stress exponent parameter of Sn- Sb alloy decrease by increasing annealing temperature[12]. The objective of the present work was to investigate microstructure, creep behavior, elastic modulus and internal friction of tin- antimony alloys.

EXPERIMENTAL WORK

In the present work, Sn_{100-x}–Sb_x (X=2.2, 10 and 50 wt.%) were melted in a muffle furnace using tin and antimony of purity better than 99.5 %. The resulting ingots were turned and re-melted four times to increase the homogeneity. From these ingots, long ribbons of about 4 mm width and ~70 μm thickness were prepared by a single roller method in air (melt spinning technique). The surface velocity of the roller was 31.4 m/s giving a cooling rate of ~3.7×10^5 K/s. The samples then cut into convenient shape for the measurements using double knife cuter. Microstructure of used specimens was performed on the flat surface of all samples using an Shimadzu X–ray Diffractometer (Dx–30, Japan) of Cu–Kα radiation with λ=1.54056 Å at 45 kV and 35 mA and Ni–filter in the angular range 2θ ranging from 0 to 80° in continuous mode with a scan speed 5 deg/min. The internal friction Q^{-1} and the elastic constants were determined using the dynamic resonance method. The value of the dynamic Young modulus E is determined by the following relationship[13–15]:

$$\left(\frac{E}{\rho}\right)^{1/2} = \frac{2\pi L^2 f_0}{kz^2}$$

Where ρ the density of the sample under test, L the length of the vibrated part of the sample, k the radius of gyration of cross section perpendicular to its plane of motion, f_0 the resonance frequency and z the constant depends on the mode of vibration and is equal to 1.8751. Plotting the amplitude of vibration against the frequency of vibration around the resonance f_0 gives the resonance curve, the internal friction, Q^{-1}, of the sample can be determined from the following relationship:

$$Q^{-1} = 0.5773\frac{\Delta f}{f_0}$$

Where Δf the half width of the resonance curve.

Creep indentation behavior of used samples was studied by Vickers microhardness tester (Model - FM-7- Japan) using load of 10 gf for indentation times up to 60 sec. The analysis of the indentation creep was done using Mulheam-Tabor method. The expression of Mulheam-Tabor[16] is:

$$-\left(n+\frac{1}{2}\right)\log H_V = \log t + B$$

H_V is the Vickers number, t is the indentation dwell time and B is the constant. If hardness is plotted versus dwell time on log-log scale, a straight line with inverse slope $-\left(n+\frac{1}{2}\right)$ is obtained

RESULTS AND DISCUSSIONS

X-ray analysis

X-ray diffraction patterns with its analysis of Sn_{100-x}–Sb_x (X=2.2, 10 and 50 wt.%) rapidly solidified alloys are shown in figure 1. Figure 1 shows that, sharp lines of body-centered tetragonal Sn phase, intermetallic compound SbSn and dissolved Sb atoms on grain

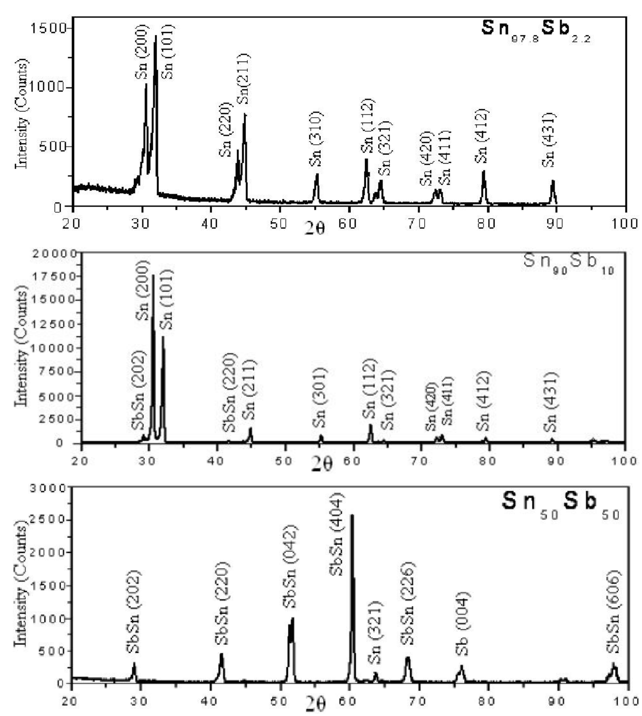

Figure 1 : X-ray diffraction patterns of Sn_{100-x}–Sb_x (X=2.2, 10 and 50 wt.%) rapidly solidified bearing solder alloys

TABLE 1 : X-ray analysis of Sn- Sb rapidly solidified bearing solder alloys

2θ	d Å	Intensity %	phase	h k l	Crystal size Å
a) $Sn_{97.8}Sb_{2.2}$					
30.6315	2.91868	76.05	Sn	200	465.1125
32.028	2.79454	100	Sn	101	525.1169
43.8622	2.06414	29.73	Sn	220	1451.588
44.9263	2.01769	51.47	Sn	211	727.9325
55.3389	1.66018	20.59	Sn	301	379.7818
62.4809	1.48649	29.55	Sn	112	262.3361
64.5053	1.44464	18.64	Sn	321	340.9827
72.4186	1.30504	10.20	Sn	420	250.1591
73.1562	1.29370	11.36	Sn	411	359.0958
79.5292	1.20528	21.65	Sn	312	583.5908
89.3676	1.09543	16.33	Sn	431	465.5777
b) $Sn_{90}Sb_{10}$					
2θ	**d Å**	**Intensity%**	**phase**	**h k l**	**Crystal size Å**
29.1104	3.06765	4.31	SbSn	202	260.655
30.5905	2.9225	100	Sn	200	220.2818
32.0363	2.79383	65.25	Sn	101	221.0621
41.5735	2.17232	1.04	SbSn	220	215.8977
44.884	2.01949	9.09	Sn	211	242.6757
55.3171	1.66078	4.3	Sn	301	227.885
62.5875	1.48421	10.47	Sn	321	248.6546
64.5052	1.44464	1.52	Sn	420	265.2194
72.2364	1.30789	3.8	Sn	411	277.6631
79.4891	1.20578	3.03	Sn	412	276.3409
89.1357	1.09768	2.32	Sn	431	290.4054
c) $Sn_{50}Sb_{50}$					
2θ	**d Å**	**Intensity %**	**phase**	**h k l**	**Crystal size Å**
29.0799	3.07079	9.74	SbSn	202	914.7121
41.5716	2.17241	17.49	SbSn	202	242.6491
51.7774	1.76567	35.08	SbSn	042	996.4023
60.4125	1.53233	100	SbSn	404	168.688
63.8037	1.45882	5.29	Sn	400	374.9948
68.1672	1.37569	14.01	SbSn	226	271.5512
76.1113	1.25065	10.38	Sb	009	216.13
97.864	1.02256	11.09	SbSn	606	361.1083

boundary/or clustered in small cluster in the Sn matrix. The analysis of x-ray diffraction patterns in TABLE (1a, b and c) show that, quantity and size of intermetallic compound SbSn increased as Sb content increased. Also all feature of formed phases, (intensity, broadness and position) changed as Sb content increase.

Mechanical properties

Elastic modulus, (E), of Sn_{100-x}–Sb_x (X=2.2, 10 and 50 wt.%) rapidly solidified alloys increased with Sb content increased as shown in TABLE 2. That is because added more a mount of Sb formed more strengthening phases, Sb and SbSn, with high elastic modulus which increased bond strength between matrix atoms.

Internal friction, (Q^{-1}), and Thermal diffusivity, (D_{th}), values of Sn_{100-x}–Sb_x (X=2.2, 10 and 50 wt.%) rapidly solidified alloys decreased with Sb content increased as shown in TABLE 2.

TABLE 2 : Elastic modulus, internal friction and thermal diffusivity of Sn- Sb rapidly solidified bearing solder alloys

Alloys	E (GPa)	Q^{-1}	D_{th} cm^2/s
$Sn_{97.8}Sb_{2.2}$	10.55	0.0463	128.08
$Sn_{90}Sb_{10}$	15.19	0.0377	99.74

Creep indentation

Creep behavior of Sn_{100-x}–Sb_x (X=2.2, 10 and 50 wt.%) rapidly solidified alloys was investigated by indentation method, Vickers hardness test, performed at room temperature. The indentation creep data are shown in figure 2 where the indentation length is plotted against the indentation time applying constant load of 10 gf. It can be seen from these figures that the indentation length increased with the loading time increased and the curves consist of two stages similar to an ordinary creep curve. The first stage of the curve records an increase in the indentation length with increased loading time, with a decreasing rate, followed by a steady-state region where indentation sizes increase linearly with time. As the hardness test is actually a compression test, fracture of the specimen dose not occurs and hence it is obviously not possible to record a third stage of the curve as opposed to what happens in an ordinary creep test.

In the Mulheam-Tabor method, figure 2, Vickers hardness number of Sn_{100-x}–Sb_x (X=2.2, 10 and 50 wt.%) rapidly solidified bearing solder alloys is plotted versus indentation time on log-log scale for the indentation data. It is observed that there exists a linear relation ship between indentation time and hardness for all conditions. The inverse slope of the resultant lines according Mulheam-Tabor method is $-\left(n+\frac{1}{2}\right)$ where n

TABLE 3 : Stress exponent of Sn- Sb rapidly solidified bearing solder alloys

Alloys	Stress exponent (n)
$Sn_{97.8}Sb_{2.2}$	3.373
$Sn_{97.8}Sb_{2.2}$	5.48
$Sn_{50}Sb_{50}$	12.57

is the stress exponent. The stress exponent values of Sn_{100-x}–Sb_x (X=2.2, 10 and 50 wt.%) rapidly solidified bearing solder alloys are given in TABLE 3. These exponent values are in the range of 5.48–12.57 depending on the composition of used alloy. The higher n values than those of the Sn matrix alloy are attributable to microstructural features such as size and distribution of strengthening phases and that is agree with the pervious results in literature. Decreasing the grain size, the grain boundary is increases and grain boundaries act as more effective barriers to dislocation movement increasing stress exponent values.

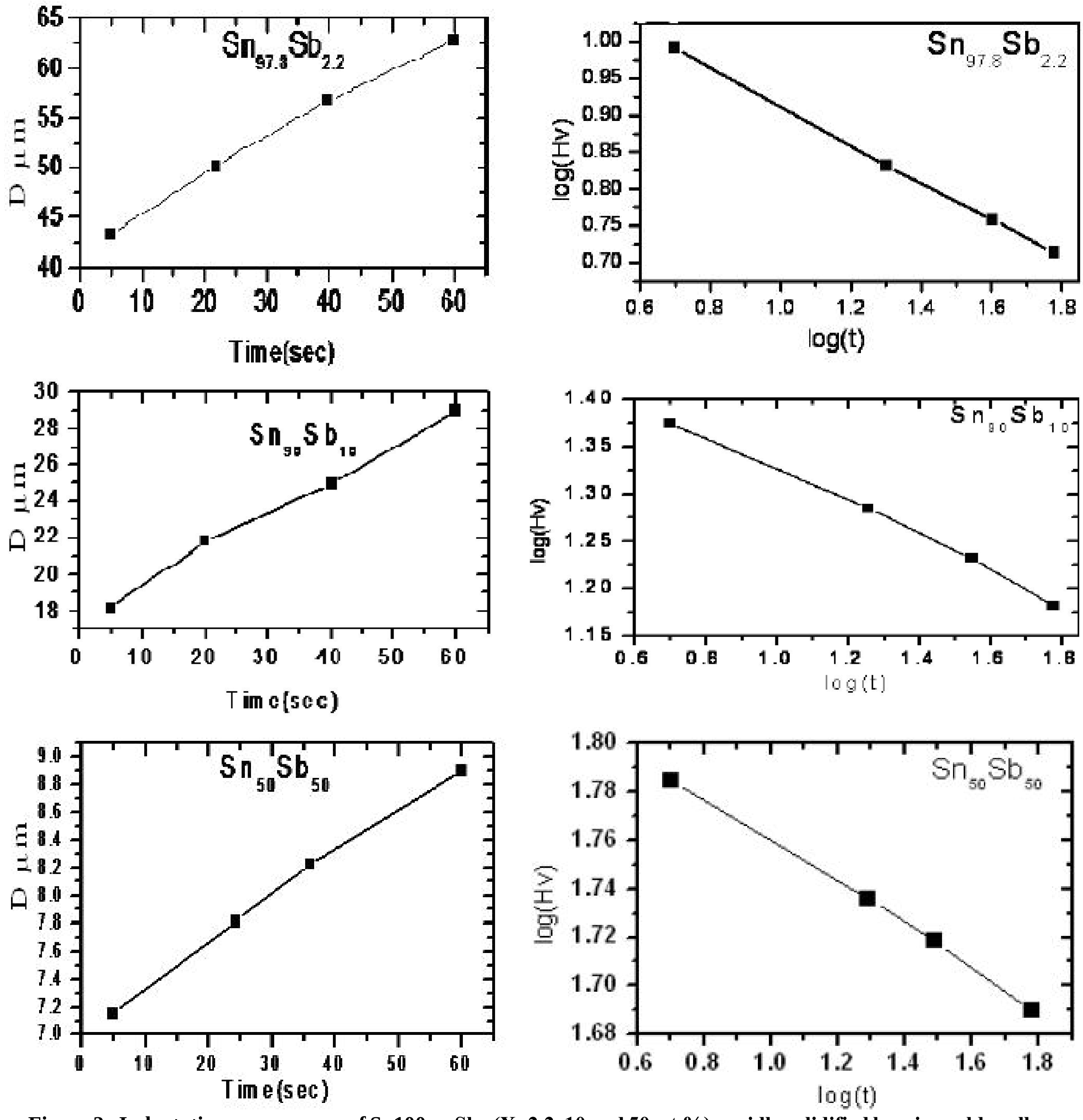

Figure 2 : Indentation creep curves of Sn100-x–Sbx (X=2.2, 10 and 50 wt.%) rapidly solidified bearing solder alloys

CONCLUSION

1. Microstructure of Sn matrix in Sn_{100-x}–Sb_x (X=2.2, 10 and 50 wt.%) rapidly solidified alloys changed with Sb content increased
2. Stress exponent values of Sn_{100-x}–Sb_x (X=2.2, 10 and 50 wt.%) rapidly solidified alloys are in the range of 5.48–12.57 dependent on its microstructural features of these alloys and agree with pervious results in literature.
3. Elastic modulus value of Sn_{100-x}–Sb_x (X=2.2, 10 and 50 wt.%) rapidly solidified alloys increased but internal friction value decreased with Sb content increased
4. Brittleness of Sn_{100-x}–Sb_x (X=2.2, 10 and 50 wt.%) rapidly solidified alloys increased with Sb increased.

REFERENCES

[1] M.Moazami Goudarzi, S.A.Jenabali Jahromi, A.Nazarboland; Investigation of characteristic of tin-based white metals, Materials and Design, **30**, 2283 **(2009)**.

[2] M.Kamal, A.Abdel-Salam, J.C.Pieri; Modification in tin-antimony alloys, J.Mater.Sci., **19**, 3880 **(1984)**.

[3] A.B.El-Bediwi; Effect of annealing and additions on dynamic mechanical properties of Sn Sb quenched alloy, Radiat.Eff.Def.Sol., **159**, 539 **(2004)**.

[4] M.Kamal, S.Mazen, A.El-Bediwi, M.El-Naggar; Radiat.Eff.Def.Sol., **467**, 157 **(2002)**.

[5] A.El-Bediwi; Effects of micro -addition on structures and properties of rapidly solidified Sn-10%Sb alloy, Radiat.Eff.Def.Sol., **158**, 475 **(2003)**.

[6] A.El-Bediwi; Effects of Cu and Ag as ternary and quaternary additions on some physical properties of $SnSb_7$ bearing alloy, Radiat.Eff.Def.Sol., **159**, 125 **(2004)**.

[7] M.Kamal, A.El-Bediwi, M.R.El-Shobaki; Influence of alloying elements on structure and some physical properties of quenched Sn-Sb alloy, Radiat.Eff.Def.Sol., **161**, 549 **(2006)**.

[8] A.El-Bediwi, A.R.Lashin, M.Mossa, M.Kamal; Micro-structure and physical properties of Sn-Sb-Cu based bearing rapidly solidified alloys, Mater.Sci.An Indian J., **6**, 45 **(2010)**.

[9] A.El-Bediwi, A.R.Lashin, M.Mossa, M.Kamal; Mater.Sci.Eng.A., **528**, 3568 **(2011)**.

[10] R.Mahmudi, A.Rezaee-Bazzaz, H.R.Banaie-Fard; J.Alloy Compd, **192**, 429 **(2007)**.

[11] R.Mahmudi, A.R.Geranmayeh, M.Bakherad, M.Allami; Mater.Sci.Eng.A., **173**, 457 **(2007)**.

[12] R.Roumina, B.Raeisinia, R.Mahmudi; Scripta Mater., **497**, 51 **(2004)**.

[13] E.Schreiber, O.L.Anderson, N.Soga; 'Elastic constant and their measurements', McGraw-Hill, New York, 82 **(1973)**.

[14] S.Timoshenko, J.N.Goddier; 'Theory of elasticity, 2nd Edition, McGraw-Hill, New York, 277 **(1951)**.

[15] K.Nuttall; J.Inst.Met., **99**, 266 **(1971)**.

[16] T.O.Mulheam, D.Tabor; J.Inst.Met., **89**, **(1960)**.